Stable and fast semi-implicit integration of the stochastic Landau–Lifshitz equation

2010 J. Phys.: Condens. Matter 22 176001

(http://iopscience.iop.org/0953-8984/22/17/176001)

IOP Publishing Journal of Physics: Condensed Matter

J. Phys.: Condens. Matter **22** (2010) 176001 (12pp) doi:10.1088/0953-8984/22/17/176001

Stable and fast semi-implicit integration of the stochastic Landau–Lifshitz equation

J H Mentink[1], M V Tretyakov[2], A Fasolino[1], M I Katsnelson[1] and Th Rasing[1]

[1] Institute for Molecules and Materials, Radboud University Nijmegen, Heijendaalseweg 135, 6525 AJ, Nijmegen, The Netherlands

[2] Department of Mathematics, University of Leicester, Leicester LE1 7RH, UK

E-mail: J.Mentink@science.ru.nl and M.Tretyakov@le.ac.uk

Received 8 February 2010, in final form 12 March 2010
Published 7 April 2010
Online at stacks.iop.org/JPhysCM/22/176001

Abstract

We propose new semi-implicit numerical methods for the integration of the stochastic Landau–Lifshitz equation with built-in angular momentum conservation. The performance of the proposed integrators is tested on the 1D Heisenberg chain. For this system, our schemes show better stability properties and allow us to use considerably larger time steps than standard explicit methods. At the same time, these semi-implicit schemes are also of comparable accuracy to and computationally much cheaper than the standard midpoint implicit method. The results are of key importance for atomistic spin dynamics simulations and the study of spin dynamics beyond the macro spin approximation.

(Some figures in this article are in colour only in the electronic version)

1. Introduction

Dynamics of magnetic materials have been theoretically studied for many years starting from the seminal work by Landau and Lifshitz [1] (see, for example, the monographs [2–4]). The current interest in this area is rapidly growing due to new important fields of application such as spintronics [5] and laser-induced ultrafast spin dynamics [6–9]. In many situations, such as the interaction of domain walls with pinning centers [10], there are atomic-scale inhomogeneities which require multiscale simulations bridging macroscopic and microscopic lengths [11]. In [12, 13] a method of *ab initio* spin dynamics was suggested relating first-principles electronic structure calculations with Landau–Lifshitz-type dynamics of classical spins within the framework of the rigid-spin approximation.

Thus, atomistic spin dynamics (ASD) simulations are important from many points of view. To do calculations at finite temperatures, there are two main approaches: a generalized Nose–Hoover (Bulgac–Kuznecov) thermal bath or Langevin (stochastic) dynamics [13]. The first method has fictitious dynamics, and hence it can be used to simulate equilibrium properties only. Langevin spin dynamics with first-principles magnetic interaction parameters has recently been implemented [14] and applied for simulating dilute magnetic semiconductors [15] and spin glasses [16]. Langevin spin dynamics are also used as a phenomenological simulation tool, not connected with first-principles theory. An implementation of this type was reported in [17] and applied to laser-induced magnetization dynamics [18].

The heart of Langevin spin dynamics simulations is integration of the stochastic Landau–Lifshitz (SLL) equation for each atomic spin. This equation is nonlinear, and analytical solutions for interacting systems exist for two spins only. In systems of interest for applications the number n of spins is typically of the order of 10^6 and the integration should be done numerically. Due to the interactions, one has to solve a system of $3n$ coupled nonlinear equations. To compute quantities in equilibrium, this very large system should be simulated over long time intervals, usually from 10 fs to 1 ns. This is a challenging computational task.

Thus, ASD requires effective numerical integrators for the SLL equation. Due to the large system size and long simulation time, such numerical methods should be on the one hand sufficiently stable and on the other hand very fast. The latter rules out the use of fully implicit integrators such as the implicit midpoint (IMP) scheme (see its application for Langevin spin dynamics, for example, in [19]). Despite its superior stability properties which allows large step sizes, typically 10 fs, IMP is slow in practice since the implicitness requires solution of

$3n$ nonlinear coupled equations at every time step. Langevin spin dynamics simulations have often been based on the Heun method [14, 17], which has the advantage of being fast in terms of the number of operations per time step. However, this method has poor stability properties, requiring a relatively small step size typically ranging from 0.01 to 1 fs, depending on the implementation. We also note that since the accuracy of the first-principles magnetic interaction parameters is limited to 10%, the accuracy of numerical methods is, to some extent, less important here than their stability (in the sense of the ability to use larger step sizes for long time simulations). Hence, both the standard implicit and explicit numerical integrators are not optimal for ASD and it is desirable to develop a numerical method that is both stable and fast. Also, ASD simulations are often used to study systems with different interactions and/or different symmetries. Therefore, in addition we should require numerical integrators for ASD to be universal in their implementation. Such a method is proposed in this paper.

As is known from the deterministic ([20–22] and the references therein) and stochastic [23–25] numerical approaches, to numerically integrate dynamical systems over long time intervals with relatively large step sizes it is advisable to preserve geometrical properties of the continuous dynamics. Therefore, one should construct and use geometrical integrators for ASD.

In the case of the deterministic Landau–Lifshitz (LL) equation, there are geometric integrators [21, 22, 26, 27] that are both stable and fast. Usually, these schemes are semi-implicit. Unlike IMP, a semi-implicit method requires only the solution of three linear coupled equations for each spin individually. However, implementation of these methods depends on symmetry and interactions in a system under consideration, which makes it difficult to use them for models with arbitrary lattice structures.

Further, semi-implicit methods for the deterministic LL equation are also considered in the review in [28]. Being based on IMP, they have the potential to combine stability and low computational costs like the geometric integrators but with the advantage of a universal implementation. In this paper we use the idea of semi-implicitness to derive new numerical methods for Langevin spin dynamics simulations which are both stable and fast and allow universal implementation. In particular, we show that, due to the enhanced stability, our semi-implicit integrator (named SIB) allows time steps a factor of 10–10^3 larger than the standard Heun method.

This paper is organized as follows. In section 2, we formulate the problem in mathematical terms, introduce the necessary notation and examine the conservation properties of the SLL equation. In section 3, we propose two new semi-implicit methods (SIA and SIB) and recall the Heun scheme and IMP. Both SIA and SIB intrinsically preserve the length of individual spins while SIB (like IMP) also possesses other conservation properties in the deterministic case. The latter is apparently the reason for the superiority of SIB which is our numerical method of choice for ASD. In section 4, we present some results of numerical experiments. We first test the considered numerical methods in the deterministic case without damping, using a simple system of two interacting spins. Then the 1D Heisenberg chain is used as a test system for the stochastic case. In section 5, we draw conclusions and recommendations for future work. Two appendices are included to provide some auxiliary knowledge of stochastic numerics and about ergodicity of the SLL equation.

2. Mathematical model

In this section we formulate the problem in mathematical terms and introduce the necessary notation. In addition, we discuss why we use the Stratonovich interpretation for the stochastic LL equation. Finally, we examine the properties of the solution of the equations under study.

The (deterministic) Landau–Lifshitz equation in dimensionless variables can be written in the form

$$\frac{\mathrm{d}X^i}{\mathrm{d}t} = -X^i \times B^i(\mathbf{X}) - \alpha X^i \times [X^i \times B^i(\mathbf{X})], \qquad i = 1, \ldots, n, \tag{1}$$

where n is the number of spins, $X^i = (X^i_x, X^i_y, X^i_z)^\top$ are three-dimensional column-vectors representing unit spin vectors[3] and $\mathbf{X} = (X^{1^\top}, \ldots, X^{n^\top})^\top$ is a $3n$-dimensional column-vector formed by the X^i; B^i is the effective field acting on spin i; $\alpha \geqslant 0$ is the damping parameter. In (1) the time is normalized by the precession frequency $\omega_{\hat{B}} = \gamma \hat{B}$, where $\hat{B}$ is some reference magnetic field strength, and the effective field $B = (B^{1^\top}, \ldots, B^{n^\top})^\top$ is also normalized by $\hat{B}$ and is given by

$$B(\mathbf{x}) = -\nabla H(\mathbf{x}), \tag{2}$$

where H is the Hamiltonian of the problem. Then

$$B^i(\mathbf{x}) = -\nabla_i H(\mathbf{x}),$$

where ∇_i is the gradient with respect to the Cartesian components of the effective magnetic field acting on spin i.

For atomistic spin dynamics, the most important contributions to the Hamiltonian are the Heisenberg exchange for the interaction between the spins H_{ex}, the Zeeman energy for the interaction with an external field H_{ext}, and the uniaxial anisotropy H_{ani} defining a preferential direction of the spins. Therefore we consider here the following Hamiltonian for our problem:

$$H = H_{\mathrm{ex}} + H_{\mathrm{ext}} + H_{\mathrm{ani}}, \tag{3}$$

where

$$H_{\mathrm{ex}}(\mathbf{x}) = -\sum_{i \neq j} J_{ij} x^i x^j, \qquad H_{\mathrm{ext}}(\mathbf{x}) = -B_0 \sum_i x^i,$$
$$H_{\mathrm{ani}}(\mathbf{x}) = K \sum_i (x^i e_K)^2.$$

Here J_{ij} are the exchange parameters, B_0 is the uniform external field, K is the strength of the anisotropy, and e_K is a unit vector that defines the anisotropy axis. Note that with these contributions to the Hamiltonian the effective fields B^i are

[3] In the paper, we follow the standard notation of the theory of stochastic differential equations and use capital letters to denote solutions of differential equations while we use small letters for the initial data and for corresponding 'dummy' variables.

linear in x. In realistic materials usually $|J_{ij}| \gg |B_0| \gg |K|$. For the exchange parameters themselves, typically $J_{i(i+1)} \gg J_{i(i+j)}$, $j > 1$, i.e. all spins interact with each other but the nearest-neighbor interactions dominate. Since all the spins interact, equation (1) involves simultaneous solution of a $3n$ system of nonlinear equations. Due to the interactions between the spins, each effective field B^i is time-dependent and equation (1) has in general no analytical solution. As a result, efficient numerical methods are required to study spin systems. In turn, the time-dependence of the effective field is usually considered as the main source of instability in the numerical integration.

In order to perform spin dynamics at finite temperature, fluctuations are included according to the Brownian motion approach for spins by adding fluctuating torques to equation (1) [29, 30]. The stochastic Landau–Lifshitz (SLL) equation is then given by

$$\frac{\mathrm{d}X^i}{\mathrm{d}t} = -X^i \times (B^i(\mathbf{X}) + b^i) - \alpha X^i \times [X^i \times (B^i(\mathbf{X}) + b^i)], \quad i = 1, \ldots, n, \tag{4}$$

where the fluctuating magnetic fields b^i are uncorrelated Gaussian white noises interpreted in the sense of Stratonovich and

$$\langle b_l^i(t)\rangle = 0, \qquad \langle b_l^i(t) b_k^j(0)\rangle = 2D\delta_{ij}\delta_{lk}\delta(t), \quad i = 1, \ldots, n, \tag{5}$$

with $\langle\cdot\rangle$ denoting ensemble averages and $l, k = x, y, z$ labeling the Cartesian coordinates, while D is the strength of the fluctuations. According to the fluctuation dissipation theorem, we choose

$$D = \frac{\alpha}{(1+\alpha^2)} \frac{k_\mathrm{b} T}{\hat{X}\hat{B}}, \tag{6}$$

where $\hat{X}$ is the (non-normalized) magnetization of each spin.

Note that (4) is a differential equation with multiplicative noise which requires us to specify in which sense we interpret the stochastic equation [31]. As said above, we use here the Stratonovich interpretation following [29]. This choice is be motivated as follows. First of all, the Stratonovich interpretation (contrary to any other one and, in particular, to the Ito interpretation) leads to preservation of the individual spin length (see (10) below) by (4), which is very important for modeling spin systems (see also a similar discussion in [19]). Further, it is natural to model a perturbation of the Landau–Lifshitz dynamics by Gaussian noise with a finite bandwidth spectrum (i.e. by a colored noise [31]), possibly with a very short correlation time. The white noise $b(t)$ in (4) has zero correlation radius (see (5)) and a spectrum with infinite bandwidth. This noise is a convenient idealization which can be viewed as an approximation of the colored noise with short correlation time. Indeed, if we consider a sequence of solutions $X_n(t)$ of the equations $\dot{X}_n^i = -X_n^i \times (B^i(\mathbf{X}_n) + b_n^i) - \alpha X_n^i \times [X_n^i \times (B^i(\mathbf{X}_n) + b_n^i)]$, where $b_n(t)$ is a sequence of Gaussian processes with correlation functions that go to the δ-function as $n \to \infty$, then $\mathbf{X}_n$ tends to the solution $\mathbf{X}$ of (4) if it is interpreted in the Stratonovich sense [32, chapter 2], [33, chapter 5]. We also note in passing that one can model a Gaussian colored noise by the Ornstein–Uhlenbeck process [31] which can be substituted in (4) instead of the white noise $b(t)$. It could be of interest to study the influence of the correlation radius on the stochastic Landau–Lifshitz dynamics. We do not pursue such questions in this paper but remark that effective numerical methods for differential equations with colored noise are available in [24, 34] which can be adapted to the SLL equation with colored noise.

Since we will exploit some results from stochastic numerics [24], which in turn follows the standard theory of stochastic differential equations, it is convenient to rewrite the SLL equation (4) in differential form [31]:

$$\mathrm{d}X^i = X^i \times a_i(\mathbf{X})\,\mathrm{d}t + X^i \times \sigma(X^i) \circ \mathrm{d}W^i(t), \qquad X^i(0) = x_0^i, \quad |x_0^i| = 1, \quad i = 1, \ldots, n, \tag{7}$$

where $W^i(t) = (W_x^i(t), W_y^i(t), W_z^i(t))^\top$, $i = 1, \ldots, n$; $W_x^i(t), W_y^i(t), W_z^i(t)$, $i = 1, \ldots, n$, are independent standard Wiener processes; $a_i(\mathbf{x})$, $\mathbf{x} \in \mathbb{R}^{3n}$, are three-dimensional column-vectors defined by

$$a_i(\mathbf{x}) = -B^i(\mathbf{x}) - \alpha x^i \times B^i(\mathbf{x}); \tag{8}$$

and $\sigma(x)$, $x \in \mathbb{R}^3$, is a 3×3-matrix such that

$$\sigma(x)y = -\sqrt{2D}y - \alpha\sqrt{2D}x \times y \tag{9}$$

for any $y \in \mathbb{R}^3$. Note that the symbol '$\circ$' in equations (7) means that the corresponding stochastic integral is interpreted in the Stratonovich sense [31]. We recall [32] (see also [31, 33]) that the Stratonovich stochastic integral can be defined as the mean-square limit of the middle Riemann sums, which, in particular, makes it evident why the midpoint scheme (see (15) below) satisfies the Stratonovich calculus.

Let us consider some properties of the solution to (7)–(9). First, the length of each individual spin is a constant of motion, i.e.

$$|X^i(t)| = 1, \qquad i = 1, \ldots, n, \quad t \geqslant 0. \tag{10}$$

Indeed, we have

$$\mathrm{d}\tfrac{1}{2}|X^i|^2 = X^i\,\mathrm{d}X^i = X^i[X^i \times a_i(\mathbf{X})]\,\mathrm{d}t + X^i[X^i \times \sigma(X^i) \circ \mathrm{d}W_i(t)] = 0.$$

Other general conservation laws of (7)–(9) and also of (1) do not exist. However, when we restrict ourselves to realistic systems, we have the damping coefficient $\alpha \ll 1$. This means that, in practice, solutions of (7)–(9) are, in a sense, close to the deterministic solutions of (1) with $\alpha = 0$. Hence the precessional motion can usually be considered as dominant. In turn, the largest contribution to the precessional motion is due to the exchange interaction. Therefore, it is relevant to examine the conservation laws for $\alpha = 0$. Since the Hamiltonian has no explicit time-dependence, energy is conserved for this case. Further, when only Heisenberg exchange is included we have for the total spin:

$$\sum_i \frac{\mathrm{d}X^i}{\mathrm{d}t} = \sum_{i \neq j} J_{ij} X^i \times X^j = \sum_{i>j} J_{ij}(X^i \times X^j + X^j \times X^i) = 0 \tag{11}$$

since $J_{ij} = J_{ji}$. We recall that the orientation of individual spins is time-dependent, which makes the effective field acting on each spin time-dependent due to the exchange interaction. However, at the same time, the symmetry of the exchange interaction ensures that the total spin is time-independent. Therefore the conservation of total spin is an important property for stable numerical integration of the exchange interaction. By the same arguments, when an external field is added, the total spin will precess in the external field:

$$\sum_i \frac{\mathrm{d}X^i}{\mathrm{d}t} = B_0 \times \sum_i X^i. \tag{12}$$

For this case, the length of the total spin is a constant of motion, as well as the component of the total spin along B_0. Hence the energy is also conserved but the transverse components of the total spin with respect to B_0 oscillate in time. When anisotropy is included, there are no conservation properties associated with the total spin. Finally, ergodicity of the solution to (7)–(9) is a relevant property. This is discussed in appendix A.

3. Numerical methods

In this section we consider numerical integrators for the stochastic Landau–Lifshitz equations (7)–(9). We first recall two existing numerical methods, one of which is explicit (the projected Heun scheme) and the other implicit (the midpoint scheme). Both are unsatisfactory since either they violate conservation laws (HeunP) or they are computationally very expensive (IMP). Therefore, in the main part of this section we present the two newly developed numerical methods (SIA and SIB). These methods are called semi-implicit and aim at combining the advantages of the existing explicit and implicit schemes.

As it is known from the deterministic ([20–22] and references therein) and stochastic ([23–25]) numerical approaches, to achieve accuracy in long time simulations (e.g. for computing ergodic limits) it is advisable to preserve the structural properties of the continuous dynamics by the approximating discrete ones. Then it is important to consider not only orders of convergence but also structural properties of numerical integrators for the SSL equation. Both convergence and structural properties of the schemes presented are discussed in section 3.3.

Throughout we use (for simplicity) a uniform discretization of a time interval $[0, t_\star]$ with step size $h = t_\star/N$. The value at the initial step is $X_0^i = x_0^i$, $i = 1, \ldots, n$, and X_k^i, $i = 1, \ldots, n$, denotes the approximate solution $X^i(t_k)$, $i = 1, \ldots, n$, to the SLL equation at time t_k, $k = 1, \ldots, N$.

3.1. Existing explicit and implicit numerical methods

3.1.1. Heun + projection (HeunP). The Heun method can be seen as a predictor–corrector method. Its prediction step, which we denote by $\mathcal{X}_k$, is the Euler approximation. The standard Heun method should be adjusted by an additional projection step which is needed to ensure that the length of each individual spin remains constant. For the SLL equations (7)–(9), the HeunP method reads

$$\begin{aligned}
\mathcal{X}_k^i &= X_k^i + hX_k^i \times a_i(\mathbf{X}_k) + h^{1/2} X_k^i \times \sigma(X_k^i)\xi_{k+1}^i, \\
&\quad i = 1, \ldots, n, \\
X^{*i}{}_{k+1} &= X_k^i + \frac{h}{2}[X_k^i \times a_i(\mathbf{X}_k) + \mathcal{X}_k^i \times a_i(\boldsymbol{\mathcal{X}}_k)] \\
&\quad + \frac{h^{1/2}}{2}[X_k^i \times \sigma(X_k^i)\xi_{k+1}^i + \mathcal{X}_k^i \times \sigma(\mathcal{X}_k^i)\xi_{k+1}^i], \\
X_{k+1}^i &= X^{*i}{}_{k+1}/|X^{*i}{}_{k+1}|, \qquad i = 1, \ldots, n, \\
&\quad k = 1, \ldots, N,
\end{aligned} \tag{13}$$

where $\boldsymbol{\mathcal{X}}_k = (\mathcal{X}_k^{1\top}, \ldots, \mathcal{X}_k^{n\top})^\top$; $\xi_{k+1}^i = (\xi_{k+1}^{i,1}, \xi_{k+1}^{i,2}, \xi_{k+1}^{i,3})^\top$; $\xi_k^{i,j}$, $j = 1, 2, 3$, $i = 1, \ldots, n$, $k = 1, \ldots, N$, are independent identically distributed (i.i.d.) random variables which can be distributed, e.g., as

$$P(\xi_k^{i,j} = \pm 1) = 1/2 \tag{14}$$

or $\xi_l^{i,j} \sim \mathcal{N}(0, 1)$. This indicates that the $\xi_l^{i,j}$, are i.i.d. Gaussian random variables with zero mean and unit variance. In equations (13) we explicitly added $i = 1, \ldots, n$ to emphasize that $\mathcal{X}_k$ has to be calculated first for all spins, before $\mathbf{X}_{k+1}$ is computed. We come back to this point in the numerical experiments (section 4).

3.1.2. Implicit midpoint (IMP). Contrary to the HeunP method, IMP (see, e.g. [24, p 45]) is implicit. For the SLL equations (7)–(9), IMP reads:

$$\begin{aligned}
X_{k+1}^i &= X_k^i + h\frac{X_k^i + X_{k+1}^i}{2} \times a_i\left(\frac{\mathbf{X}_k + \mathbf{X}_{k+1}}{2}\right) \\
&\quad + h^{1/2}\frac{X_k^i + X_{k+1}^i}{2} \times \sigma\left(\frac{X_k^i + X_{k+1}^i}{2}\right)\xi_{k+1}^i, \\
&\quad i = 1, \ldots, n, \quad k = 1, \ldots, N,
\end{aligned} \tag{15}$$

where $\xi_{k+1}^i = (\xi_{k+1}^{i,1}, \xi_{k+1}^{i,2}, \xi_{k+1}^{i,3})^\top$; $\xi_k^{i,j}$, $j = 1, 2, 3$, $i = 1, \ldots, n$, $k = 1, \ldots, N$, are i.i.d. random variables which can be distributed according to (14), for example. Alternatively, we can choose $\xi_k^{i,j}$ being distributed as the ξ_h defined below (see [23, 24]). Let $\zeta \sim \mathcal{N}(0, 1)$ be a Gaussian random variable with zero mean and unit variance. We define

$$\xi_h = \begin{cases} \zeta, & |\zeta| \leqslant A_h, \\ A_h, & \zeta > A_h, \\ -A_h, & \zeta < -A_h, \end{cases} \tag{16}$$

where $A_h = \sqrt{2|\ln h|}$. We note that if one takes $\xi_k^{i,j} \sim \mathcal{N}(0, 1)$, IMP can, in general, diverge (see a counter-example in [23, 24]).

3.2. New semi-implicit numerical methods

Here we propose two new semi-implicit integration schemes, simply called semi-implicit A (SIA) and semi-implicit B (SIB). In the spirit of the review [28], they are called semi-implicit since they require only to solve n, or $2n$ in the case of the

SIB scheme, linear 3×3 systems at each time step, which can be done analytically. The starting point for derivation of the semi-implicit methods is the IMP scheme. To reduce the degree of implicitness, we replace $\mathbf{X}_{k+1}$ in the argument of a_i and σ in IMP by a predictor $\boldsymbol{\mathcal{X}}_k$. As a consequence, resolving the implicitness at each time step is simplified (in comparison to IMP) to solving a linear 3×3 system per spin that is independent of the interactions between the spins. The difference between SIA and SIB is the choice for $\boldsymbol{\mathcal{X}}_k$. Both semi-implicit methods have effectively the same computational cost as explicit schemes.

3.2.1. Semi-implicit scheme A (SIA). Similar to the HeunP method, for the SIA scheme we take the Euler approximation for the predictor $\boldsymbol{\mathcal{X}}_k$. The SIA method for the SLL equation reads

$$\begin{aligned}
&\mathcal{X}_k^i = X_k^i + hX_k^i \times a_i(\mathbf{X}_k) + h^{1/2} X_k^i \times \sigma(X_k^i)\xi_{k+1}^i, \\
&\qquad i = 1, \ldots, n, \\
&X_{k+1}^i = X_k^i + h\frac{X_k^i + X_{k+1}^i}{2} \times a_i\left(\frac{\mathbf{X}_k + \boldsymbol{\mathcal{X}}_k}{2}\right) \\
&\qquad + h^{1/2}\frac{X_k^i + X_{k+1}^i}{2} \times \sigma\left(\frac{X_k^i + \mathcal{X}_k^i}{2}\right)\xi_{k+1}^i, \\
&\qquad i = 1, \ldots, n, \quad k = 1, \ldots, N,
\end{aligned} \tag{17}$$

where $\xi_{k+1}^i = (\xi_{k+1}^{i,1}, \xi_{k+1}^{i,2}, \xi_{k+1}^{i,3})^\top$; $\xi_l^{i,j}$ are i.i.d. random variables as in IMP (15) (the same two possibilities).

3.2.2. Semi-implicit scheme B (SIB). SIA can be viewed as a second iteration for the implicit equation due to IMP. As the zero approximation of $\mathbf{X}_{k+1}$, we took $\mathbf{X}_k$ and then the second iteration was constructed so that the length of individual spins is preserved. One can see that the first iteration (or in other words the prediction step) of SIA does not preserve the spin length. We are therefore proposing the SIB method which keeps the spin length conserving IMP structure at both iterations and, according to our numerical tests (see section 4), this modification is crucial for the performance of the semi-implicit schemes.

The SIB method for the SLL equation reads

$$\begin{aligned}
&\mathcal{X}_k^i = X_k^i + h\frac{X_k^i + \mathcal{X}_k^i}{2} \times a_i(\mathbf{X}_k) \\
&\qquad + h^{1/2}\frac{X_k^i + \mathcal{X}_k^i}{2} \times \sigma(X_k^i)\xi_{k+1}^i, \qquad i = 1, \ldots, n, \\
&X_{k+1}^i = X_k^i + h\frac{X_k^i + X_{k+1}^i}{2} \times a_i\left(\frac{\mathbf{X}_k + \boldsymbol{\mathcal{X}}_k}{2}\right) \\
&\qquad + h^{1/2}\frac{X_k^i + X_{k+1}^i}{2} \times \sigma\left(\frac{X_k^i + \mathcal{X}_k^i}{2}\right)\xi_{k+1}^i, \\
&\qquad i = 1, \ldots, n, \quad k = 1, \ldots, N,
\end{aligned} \tag{18}$$

where $\xi_{k+1}^i = (\xi_{k+1}^{i,1}, \xi_{k+1}^{i,2}, \xi_{k+1}^{i,3})^\top$; $\xi_l^{i,j}$ are i.i.d. random variables as in IMP (15) (the same two possibilities).

Remark. One can continue the process and make several iterations for the implicit equation due to IMP; for example, in our tests about ten iterations were sufficient to resolve the implicitness up to the machine accuracy. However, in practice the use of several iterations would be too computationally expensive while SIB already demonstrates stability and accuracy comparable with IMP.

3.3. Properties of the methods

We start by examining convergence of the methods presented in this section and then discuss some conservation properties. For completeness, in appendix B we recall some generic facts about stochastic numerics [24].

All four methods considered in this section are of weak order 1 for both choices of the distributions of $\xi_k^{i,j}$ (discrete and continuous). If $\xi_l^{i,j} \sim \mathcal{N}(0, 1)$, then HeunP is also of mean-square order $1/2$. IMP, SIA, and SIB are of mean-square order $1/2$ if $\xi_k^{i,j}$ have the cut-off Gaussian distribution (16). These convergence properties are proved using the standard results [24, chapters 1 and 2]. In the deterministic case (i.e. $D = 0$) all four methods are of order 2.

Note that in this paper we limit ourselves to methods of weak order 1 and of mean-square order $1/2$. The system (7)–(9) has noncommutative noise (see the definition in, e.g., [24, p. 28]). Then mean-square methods of orders higher than $1/2$ require simulation of multiple Ito integrals which is computationally expensive. It is possible to construct higher order weak methods for (7)–(9) but, due to the multiplicative, noncommutative nature of the noise, they would be too complicated and they are not considered here. We also note that the problem with multiplicative noise can be circumvented by rewriting the SLL equation in spherical coordinates, for which the system is Hamiltonian and the noise becomes additive, but then numerical difficulties arise when the polar angle is close to 0 or π.

When α is small, the SLL equations (7)–(9) is a system with small multiplicative noise. In this case the weak sense errors of all the methods considered in this section are of order $O(h^2 + \alpha^2 h)$ [35], [24, chapter 3]. The smallness of the noise can be further exploited to construct high accuracy but low order efficient methods following the recipe from [35, 24].

We now discuss *conservation properties* of the schemes. The HeunP method (13) has only one conservation property—norm-preservation which is due to the projection step. Heun without the projection step would conserve the total spin but then violates norm-preservation. Omitting the projection step also gives very poor results for the interaction with an external magnetic field. In practice the projection step can be exploited for error control. Energy is not conserved by HeunP when $\alpha = 0$. HeunP has the advantage of being very flexible, its implementation is independent of the symmetry of the system and types of interactions used. The method is also fast since integration can be done for each spin separately.

Due to the structure of IMP, the difference $X_{k+1}^i - X_k^i$ is always perpendicular to $X_k^i + X_{k+1}^i$. Therefore $(X_k^i + X_{k+1}^i)(X_{k+1}^i - X_k^i) = 0$ and hence $|X_{k+1}^i|^2 = |X_k^i|^2$, i.e. the length of each spin is exactly preserved by IMP without any need of projection. In the deterministic case with $\alpha = 0$ and under only the Heisenberg exchange, IMP conserves the total

spin. The proof follows directly from equation (11), replacing $\mathrm{d}X^i/\mathrm{d}t$ by $X^i_{k+1} - X^i_k$ and X^i by $(X^i_k + X^i_{k+1})/2$. The total energy conservation for the case of $\alpha = 0$ can be proven similarly. Preservation of all the main structural properties of the SLL equation by IMP comes at a cost. Since all spins are coupled, a system of $3n$ nonlinear algebraic equations has to be solved at each time step. This is a major limitation for application of IMP to atomistic spin dynamics, where the number of spins is typically of order $n = 10^6$. Some further remarks on conservation properties of both HeunP and IMP in the deterministic case are given in [21].

The SIA method is very close to the HeunP method. However, unlike the HeunP method SIA preserves the constraint $|X^i(t)| = 1$ exactly, without the need for projection. This follows directly from the observation that the norm conservation of each spin is independent of the point at which a_i and σ are evaluated. Let us now look at SIA in the deterministic case with $\alpha = 0$. Regarding total spin, the relevant symmetry property is

$$\frac{X^i_k + X^i_{k+1}}{2} \times \frac{X^j_k + \mathcal{X}^j_k}{2} + \frac{X^j_k + X^j_{k+1}}{2} \times \frac{X^i_k + \mathcal{X}^i_k}{2} \neq 0,$$

which is violated since the Euler approximation for $\mathcal{X}^i_k$ depends only on the orientation of the spins at the current time step ($\mathbf{X}_k$) but not on $\mathcal{X}^i_k$, whereas X^i_{k+1} is also determined by the value X^i_{k+1} itself. Owing to this difference, for $\alpha = 0$ the total spin cannot be preserved by SIA. Also, the energy is not a conserved quantity by SIA and the scheme introduces numerical damping. Hence SIA has the same conservation properties as HeunP, and it is of interest to investigate whether the built-in norm conservation is sufficient to improve stability properties.

Unlike SIA, SIB has the norm-conserving midpoint structure for both X^i_k and $\mathcal{X}^i_k$. In the case of a two-spin deterministic system with $\alpha = 0$ we proved analytically that both energy and total spin are conserved quantities of SIB. Hence for this system SIB has the same conservation properties as IMP. At the same time, implementation-wise very little additional computational effort is required by SIB compared to HeunP and SIA. Hence it is of interest to compare the performance of SIB with SIA, in particular to investigate the influence of preservation of norm conservation and preservation of deterministic conservation laws on the stability properties of the methods. As our numerical experiments (see section 4) suggest, SIB outperforms SIA while SIA is only slightly better than HeunP. This observation implies, in particular, that built-in norm conservation alone is not sufficient to obtain superior numerical integrators for ASD and preservation of other structural properties of the SLL equation should guide one in constructing effective numerical methods.

4. Numerical experiments

In this section, we compare performance of the integrators introduced in the previous section using two model problems. In section 4.1, we present some results of the experiments in the deterministic case without damping (i.e. $\alpha = 0$), to illustrate the conservation properties of the numerical methods. In section 4.2, we consider the stochastic case using the 1D Heisenberg chain as a test system. We show that the methods that preserve the deterministic integration laws give rise to a more stable integration for the stochastic spin dynamics.

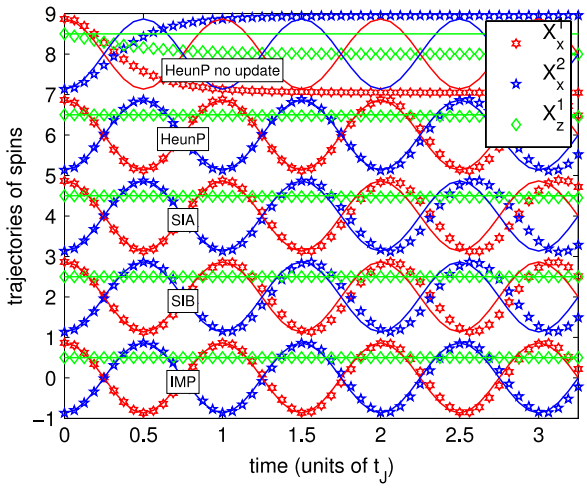

Figure 1. Comparison of the explicit HeunP, implicit IMP and semi-implicit methods SIA and SIB for the deterministic case $\alpha = 0$. The trajectory of two interacting spins is shown by plotting the x components of the two spins and one z-component. Solid lines indicate the analytical solution. The upper panel shows that without simultaneous update of the effective field the integration is very unstable. IMP demonstrates the best performance. All methods introduce errors in the precession period $t_J = 2\pi/J$ corresponding to the initial condition. For the purpose of illustration, a large step size $h = 1/16$ is used.

4.1. Two interacting spins

In order to illustrate the conservation properties of the numerical schemes related to the deterministic precessional motion, we choose the simple case of two interacting spins with equal length $|X^1| = |X^2| = 1$. As a result of the exchange interaction, the spins rotate around a common axis, where the precession frequency is given by $\omega_J = 2J\cos\theta/2$ with the angle θ between the spins and the Heisenberg exchange parameter J.

First, we emphasize the relevance of simultaneously updating the effective field. Due to the interaction, the effective field acting on each spin is determined by the other spin. Therefore, when using a predictor–corrector method like HeunP, it is highly relevant to simultaneously update the effective fields after the prediction step before calculating the correction step. Hence, the correction step is computed taking into account that $a_i(\mathcal{X}_k)$ depends on $\mathcal{X}^{j\neq i}_k$ and not on $\mathcal{X}^i_k$ alone. Therefore, at each time step the effective field must be computed twice. By its design, a predictor–corrector method must be implemented in this way, otherwise it will, as a rule, become a scheme of lower order. Figure 1 shows the computed trajectory with and without simultaneous update for the HeunP method. To achieve a comparable accuracy without a simultaneous update of the effective field, the step size should be decreased by a factor of 10^2–10^3.

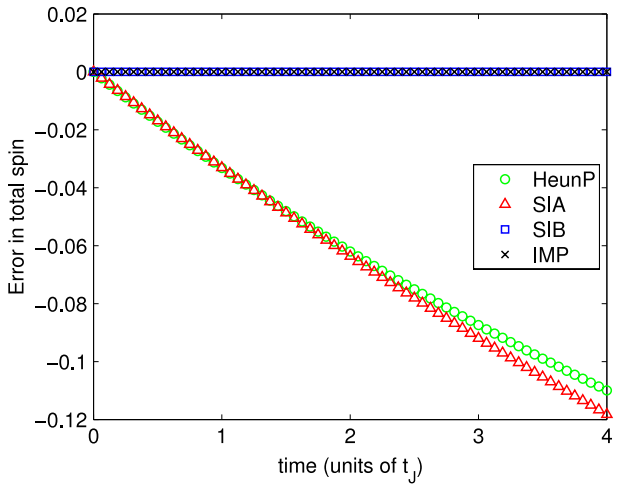

Figure 2. Conservation of total spin for HeunP, IMP, SIA, and SIB. The figure shows the error in the total spin for the same system as in figure 1. Both IMP and SIB preserve the total spin up to machine precision, whereas SIA and HeunP introduce a numerical damping. Here $t_J = 2\pi/J$ is the precession period.

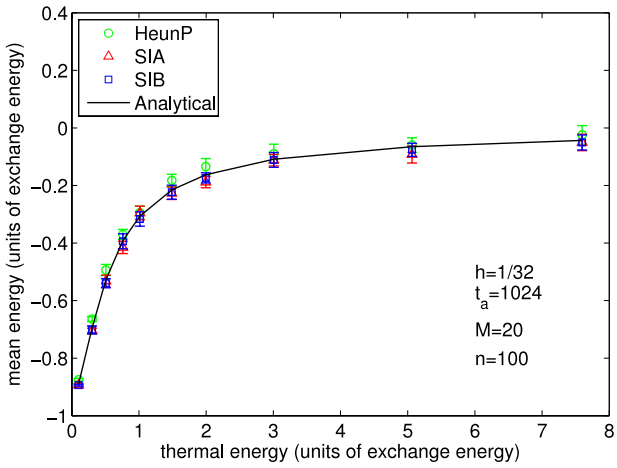

Figure 3. Temperature check of the semi-implicit methods SIA and SIB compared with the explicit HeunP method. Shown is the mean energy per spin of the 1D Heisenberg chain, as a function of temperature, computed with the parameter values shown at the bottom. All the schemes demonstrate reasonable agreement with the analytical result (19).

In the four lowest panels of figure 1 we compare the considered integrators implemented with simultaneous update of the effective fields. For illustration purposes, a large step size is used ($h = 1/16$). For small times, all methods show reasonable agreement with the analytical solution, but IMP clearly has the best performance for this system. However, even IMP, which preserves the conservation laws intrinsically, introduces errors in the precession frequency. Since these errors do not affect the conservation properties of the methods, we do not consider them in detail.

Next, we compare the conservation properties of the considered methods for the two-spin system. To this end, figure 2 shows the error in the total spin as a function of integration time. Both SIB and IMP exactly conserve the total spin, whereas HeunP and SIA have numerical dissipation. For clarity, only the z-component of the total spin is plotted. The errors in the x- and y-components of the total spin are much smaller since the numerical errors in the x, y motion of the individual spins cancel each other due to the symmetry.

Despite the fact that SIA conserves the norm of each spin exactly, the numerical damping is slightly larger than for HeunP. Both their errors are strongly dependent on the initial condition. When the spins are almost parallel, HeunP has a larger numerical error than SIA since the projection step transforms a larger amount of transverse motion to longitudinal motion. In the case of figure 2 an initial condition with $\theta_0 = 120°$ is used, which is closer to anti-parallel motion and, therefore, HeunP has a smaller error than SIA.

For this simple two-spin system, the energy and total spin are directly related: $(X_k^1 + X_k^2)^2 = (X_k^1)^2 + (X_k^2)^2 + 2X_k^1 X_k^2 = 2 + E_k/J$. Hence both SIB and IMP conserve energy, whereas both HeunP and SIA dissipate energy. For larger systems with only nearest-neighbor interactions, SIB conserves total spin and energy like IMP as well, while obviously SIB requires much less computational effort than IMP. The conservation properties of SIB can be proven analytically but this is beyond the scope of the present paper.

In conclusion, the results of the numerical experiments with two interacting spins and $\alpha = 0$ show that both HeunP and SIA introduce numerical errors in the conserved quantities whereas SIB and IMP preserve the total spin and energy of the test system.

4.2. 1D Heisenberg chain

In this section we compare the semi-implicit integration schemes with the explicit and implicit methods in the stochastic case. The simplest model of classical interacting spins is the 1D Heisenberg chain with nearest-neighbor interactions. For this system, an analytical expression for the mean energy per spin is available [36, 37]:

$$\bar{H}_{\text{analytic}} \equiv \frac{\langle H_{\text{ex}} \rangle}{2nJ} = \left(1 - \frac{1}{n}\right)\left(\frac{k_b T}{2J} - \coth\left(\frac{2J}{k_b T}\right)\right). \quad (19)$$

This expression gives us a convenient way to check how accurately the temperature of the system is reproduced in simulations using the numerical methods from section 3. Note that $\bar{H} \to -1 + 1/n$ as the temperature $T \to 0$ since we have normalized the energy with the number of spins n and the interaction energy of two spins $2JX^1X^2$ tends to $2J$ when the temperature goes to zero.

The comparison of the HeunP method with the semi-implicit schemes for the temperature is shown in figure 3 for step size $h = 1/32$, damping $\alpha = 0.1$, exchange parameter $J = 1$, spin length $|X^i| = 1$, and number of spins $n = 100$. The random variables used in the numerical schemes are simulated according to the cut-off Gaussian distribution (16). At a time step k the sample average $\hat{H}_k$ for the energy H per spin is computed as

$$\hat{H}_k = \frac{1}{M}\sum_{m=1}^{M} \frac{H_{\text{ex}}(\mathbf{X}_k^{(m)})}{2nJ}, \quad (20)$$

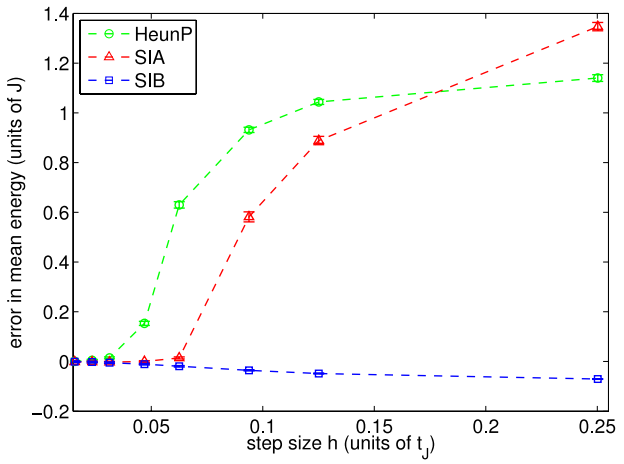

Figure 4. Stability of the semi-implicit methods SIA and SIB compared with the explicit HeunP method. The figure shows the error in the mean energy as a function of the step size h for the lowest temperature considered in figure 3, $k_bT/(2J) = 0.1$. It is found that SIB remains stable up to four steps per precession period $t_J = 2\pi/(2J)$, while SIA and HeunP become unstable and produce unreliable results.

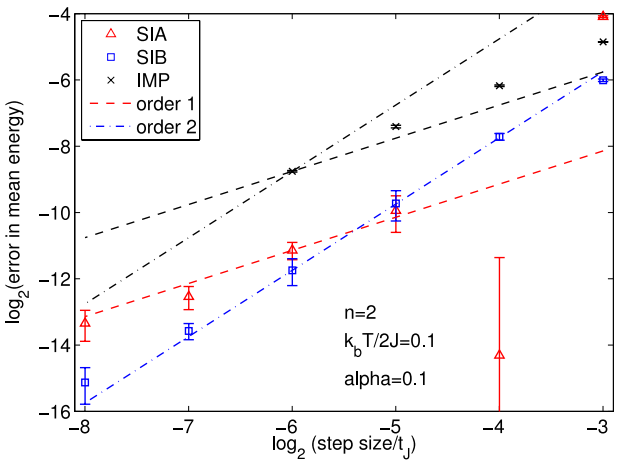

Figure 5. Comparison of the semi-implicit methods SIA and SIB with the fully implicit IMP. The figure shows the weak order convergence of SIA, SIB, and IMP schemes for the mean energy per spin. Both axes are logarithmic with base 2. For small enough step size, the slope gives the order of convergence. Surprisingly, both SIA and SIB are more accurate than IMP. Moreover, SIB shows a higher order convergence than IMP. Here $t_J = 2\pi/(2J)$ indicates the reference precession period.

where $\mathbf{X}_k^{(m)}$ are independent realizations of $\mathbf{X}_k$ obtained by a numerical scheme (see also appendix B). The corresponding standard deviation σ_{H_k} is also computed. In the experiment an ensemble of $M = 20$ independent trajectories was used. The values plotted in figure 3, with the 95% confidence intervals determined by the standard deviation, were obtained after equilibrating the system for a time $t_a = 1024t_J$ long enough for the system to be sufficiently close to equilibrium. Here $t_J = 2\pi/(2J)$ is the reference precession period for (almost) parallel spins. We find that both HeunP and the semi-implicit schemes show reasonable agreement with the analytical results, indicating that they obey the Stratonovich interpretation rule as expected.

The next question is which method is more accurate. Figure 3 shows that SIB is consistent with the analytical solution at all data points. On the contrary, HeunP and SIA show slight discrepancies. To investigate this more accurately, we study the numerical error by varying the step size. For illustration we used the lowest temperature $k_bT/(2J) = 0.1$. The results are shown in figure 4.

It is found that SIB outperforms both SIA and HeunP, and SIB remains stable down to only four steps per precession period. At such a large step size, SIA and HeunP are unstable though SIA performs slightly better than HeunP. Note that in physical units, with the exchange energy $J\hat{X}^2 = 1$ mRyd, $\hat{X} = 1\mu_{\text{Bohr}}$, four steps per precession period corresponds to a step size of about 20 fs. Hence, for SIB the step size is only limited by the precession period of the spins, and there is no need to decrease the step size to preserve the conservation laws accurately enough. This should be compared with the step size of 10 as, which was reported in [14], resulting in an enormous improvement of a factor of 2×10^3 in the allowed step size. However, the mentioned implementation of ASD in [14] is based on HeunP without the simultaneous update of the effective field. As follows from figures 1 and 4, when the effective field is properly updated, HeunP also allows a larger step size. However, the increase is limited to about 2 fs for the system studied here. Compared to HeunP, SIA has only slightly better stability properties, which we attribute to the intrinsic norm conservation. The superior stability properties of SIB can apparently be explained by its built-in deterministic conservation properties. For the system studied here, SIB allows step sizes by about a factor of 10 larger than HeunP and by about a factor of 5 larger than SIA.

Let us now compare the performance of the semi-implicit methods with the fully implicit IMP. The 1D Heisenberg chain is not convenient for this purpose, unless we choose a very small number of spins. In addition, for this comparison stability is not the major issue since we already know that the step size of SIB is limited only by the precession period. Therefore we are more interested in the intrinsic properties of the integrators that are independent of the system under study. Hence the relevant property here is the convergence of the semi-implicit and IMP schemes. To reduce computational costs of the experiment, we again use a system with only two spins.

To experimentally observe the order of convergence, a small statistical error is needed. To this end, a combination of ensemble and time averaging was used. As before, for an ensemble with M trajectories, we let the system equilibrate for a time $t_a = 2048t_J$. Subsequently, the equilibrated sample mean $\hat{H}_k$ (see (20)) is calculated for a time $t_b = 6144t_J$. The calculated values of $\hat{H}_k$ are then divided in $P = 8$ subsets of length $L = t_b/P = 768t_J$ and in each subset the time mean $\check{H}_p$ is computed. Eventually, the total mean $\check{H}$ is the average of the time means over the P subsets and its statistical error Δ is estimated by two standard deviations of $\check{H}_p$ divided by $\sqrt{P}$, which gives half of the length of the 95% confidence intervals for $\check{H}$. The results are presented in figure 5.

Table 1. The values of error in the mean energy $\epsilon = \check{H} - \bar{H}_{\text{analytic}}$ and the corresponding statistical error Δ for the considered schemes. In each consecutive row the step size is smaller by a factor of 2.

		HeunP		SIA		SIB		IMP	
h	M	ϵ	Δ	ϵ	Δ	ϵ	Δ	ϵ	Δ
1.251×10^{-1}	2^4	4.23×10^{-1}	1.1×10^{-3}	5.87×10^{-2}	1.1×10^{-3}	-1.55×10^{-2}	4.1×10^{-4}	-3.46×10^{-2}	1.3×10^{-4}
6.255×10^{-2}	2^5	2.71×10^{-2}	6.0×10^{-4}	-4.92×10^{-5}	3.3×10^{-4}	-4.76×10^{-3}	3.3×10^{-4}	-1.38×10^{-2}	2.3×10^{-4}
3.128×10^{-2}	2^7	1.84×10^{-3}	4.5×10^{-4}	-1.02×10^{-3}	3.7×10^{-4}	-1.18×10^{-3}	3.6×10^{-4}	-5.77×10^{-3}	1.4×10^{-4}
1.564×10^{-2}	2^{12}	-9.74×10^{-6}	8.1×10^{-5}	-4.43×10^{-4}	7.9×10^{-5}	-2.92×10^{-4}	5.9×10^{-5}	-2.31×10^{-3}	4.0×10^{-5}
7.819×10^{-3}	2^{16}	-9.55×10^{-5}	3.9×10^{-5}	-1.68×10^{-4}	4.0×10^{-5}	-8.20×10^{-5}	1.4×10^{-5}		
3.909×10^{-3}	2^{17}	-8.24×10^{-5}	3.0×10^{-5}	-9.62×10^{-5}	3.0×10^{-5}	-2.79×10^{-5}	1.1×10^{-5}		

Note that for this small system no instabilities appear in SIA, and this method shows the first weak order convergence as expected. Surprisingly, SIB demonstrates a second order convergence, which might be related to the fact that the energy is a conserved quantity for $\alpha = 0$. This means that for the energy only numerical errors from the damping term show up, hence the convergence for the energy in the stochastic case might be better than the convergence for a general quantity. The small error for SIA at the smallest time step but one in figure 5 is caused by the change in sign of the error. The error values are given in table 1. Here also the data for HeunP are provided. HeunP is not shown in figure 5 since it appears to be in the asymptotic regime only for the smallest time steps. We note that there is a sign change of the HeunP error, which is the reason for its small error at $h = 1.564 \times 10^{-2}$. IMP is very costly for a large ensemble, therefore the two smallest step sizes were not computed.

In general, the performance of SIB in the experiments has been better than SIA. Interestingly, despite the excellent stability of IMP, the accuracy of IMP in the stochastic case lags behind SIB and SIA. This is a good example of a situation when a method with better stability does not necessarily have a better accuracy. It was also observed in the deterministic case with damping that SIB sometimes shows better accuracy than IMP. This implies that in the case of damped motion the numerical integration error of IMP can be larger than for SIB, as is observed in the stochastic case. These results show that at least for the systems considered here, SIB has the same stability properties as IMP, but at considerably lower computational costs.

In conclusion, we find that in the stochastic case the SIB method, with built-in deterministic conservation laws, is more stable and has smaller numerical errors than both the SIA and the HeunP methods. Surprisingly, in the stochastic case SIB is even better than IMP in terms of accuracy and convergence. SIA performs only slightly better than HeunP in the stochastic case, and from this we find that norm conservation is not the most important criterion for stable numerical integration of the SLL equation. Hence, SIB combines the advantages of both HeunP and IMP, being both fast and stable as well as universal. For systems with only nearest-neighbor interactions, SIB allows step sizes a factor of 10 larger than the popular HeunP scheme, and a factor of 2×10^3 larger than the HeunP method without simultaneous update of the effective field. Since in practice nearest-neighbor interactions dominate, SIB is expected to also be advantageous for systems with more than nearest-neighbor interactions.

5. Conclusions and outlook

In this paper we introduced two new semi-implicit integrators (SIA and SIB) for stochastic atomistic spin dynamics (ASD) simulations. These schemes combine the advantages of the standard explicit projected Heun method (HeunP) and the fully implicit midpoint method (IMP). The semi-implicit methods are as fast as explicit schemes since they require only the solution of three linear coupled equations for each spin individually and therefore they are effectively explicit. For stability, the most important conservation law is apparently the preservation of the total spin for the case without damping. Like IMP, SIB preserves this conservation law for the dominant interactions in the system and the stability properties of SIB are comparable with IMP. SIA, which has norm conservation built in but not the deterministic conservation laws, shows only slightly better stability than HeunP in the stochastic case. Therefore, we recommend the use of SIB for ASD simulations.

Owing to the enhanced stability, larger step sizes can be used with SIB. From our numerical experiments we can conclude that the step size can be increased by a factor of about 10 compared to the explicit HeunP. For SIB, the step size is only limited by the precession frequency of the individual atomic spins in the exchange field, which allows for step sizes of about one-quarter of the precession period which can be as large as 20 fs. This value of the step size has to be compared with the 10 as that was reported for a standard implementation of ASD simulations [14], which is based on the HeunP method without the simultaneous update of the effective field. Hence, the factor of 2×10^3 improvement can be attributed to a proper update of the effective field and built-in conservation of the total spin for SIB. Interestingly, numerical experiments indicate that SIB can also be more accurate than IMP in the stochastic case. Further checks for the stochastic case, including larger systems, more complicated interactions, and correlations, will be discussed in a subsequent paper.

Future work should study the conservation properties of SIB in more detail in order to give a further explanation of its excellent behavior. It would also be of interest to obtain a method obeying conservation laws for systems with more complicated interactions (e.g. next-nearest-neighbor, anisotropy). In addition, one might exploit the fact that the damping motion and the precessional motion are always perpendicular, which can potentially be used to design an integrator that exactly dissipates energy as in continuous dynamics. Another direction which we can pursue in

future is to derive stochastic counterparts of the geometric integrators proposed in [21, 22] for deterministic Landau–Lifshitz equations. Although they lack flexibility to deal with models with arbitrary lattice structures, such geometric integrators are expected to be highly efficient when it is sufficient to include only nearest-neighbor interaction in the stochastic model. Our method can also be of value for micromagnetic simulations, and we expect that similar techniques can be exploited for other physical systems where interactions between particles are governed by a global conservation law, e.g. systems based on diffusion equations such as the Schrödinger equation.

Acknowledgments

This work was partially supported by the Nederlandse Organisatie voor Wetenschappelijk Onderzoek (NWO) and de Stichting voor Fundamenteel Onderzoek der Materie (FOM). The authors thank O Eriksson, Uppsala University, Sweden, for computational support.

Appendix A

In this appendix we discuss the ergodicity of the solution $\mathbf{X}(t)$ to (7)–(9). For the solution $\mathbf{X}(t)$ of (7)–(9) we will also use the notation $\mathbf{X}_{\mathbf{x}}(t)$ to reflect the dependence on the initial condition $\mathbf{X}_{\mathbf{x}}(0) = \mathbf{x}$. Taking into account (2) and (3), we observe that the coefficients of (7)–(9) are smooth functions and due to (10) they remain bounded for all $t \geqslant 0$.

One can show [33, 38] that for $D > 0$ and $\alpha > 0$ the process $\mathbf{X}(t)$ is ergodic, i.e. there exists a unique invariant measure μ of $\mathbf{X}$ and independently of $\mathbf{x} \in \mathbb{R}^{3n}$ there exists the limit

$$\lim_{t\to\infty} \langle \varphi(\mathbf{X}_{\mathbf{x}}(t)) \rangle = \int \varphi(\mathbf{x})\, \mathrm{d}\mu(\mathbf{x}) \equiv \varphi^{\mathrm{erg}} \qquad \text{(A.1)}$$

for any function $\varphi(x)$ with polynomial growth at infinity. Indeed, the solution $\mathbf{X}(t)$ of (7)–(9) belongs to the compact space due to (10). Then to prove ergodicity, it is enough to show that there is sufficient mixing. When $\alpha = 0$, the stochastic perturbation is only precessional and, in general (e.g. for constant B), the process $\mathbf{X}(t)$ is not ergodic. When $\alpha > 0$, the stochastic perturbation acts in all directions on the spheres $|x^i| = 1$ and so ensures a mixing sufficient for the ergodicity.

We also recall the ergodic theorem, which gives the equivalence between the ensemble and time averaging:

$$\lim_{t\to\infty} \frac{1}{t} \int_0^t \varphi(\mathbf{X}_{\mathbf{x}}(s))\, \mathrm{d}s = \varphi^{\mathrm{erg}} \qquad \text{almost surely,} \qquad \text{(A.2)}$$

where the limit does not depend on $\mathbf{x}$.

Further, the invariant measure associated with the solution $\mathbf{X}(t)$ of (7)–(9) is Gibbsian with the density

$$\rho(\mathbf{x}) \propto \exp(-\beta H(\mathbf{x})), \qquad \text{(A.3)}$$

where $\beta = \hat{X}\hat{B}/(k_{\mathrm{B}}T) > 0$ is the inverse temperature if we choose the noise intensity D as in (6). To check that (A.3) is the density of the invariant measure for (7)–(9) and (6), one needs to verify that this $\rho(\mathbf{x})$ is the solution of the stationary Fokker–Planck equation for (7)–(9), (6). Such calculations are available, e.g. in [39].

Appendix B

In this appendix we recall some generic facts from stochastic numerics [24]. In particular, we define the weak order of convergence of numerical methods for stochastic differential equations (SDEs) and discuss errors arising in computing ergodic limits.

Let us introduce a system of SDEs of a general form

$$\mathrm{d}X = \alpha(X)\, \mathrm{d}t + \sum_{l=1}^{r} \beta_l(X)\, \mathrm{d}W_l(t), \qquad X(0) = x, \quad \text{(B.1)}$$

where X, α, β_l are d-dimensional column-vectors and $W_l(t)$, $l = 1, \ldots, r$, are independent standard Wiener processes. Consider a numerical method for (B.1) based on the one-step approximation:

$$X_{t,x}(t+h) \simeq \bar{X}_{t,x}(t+h) = x + A(t, x, h; \xi), \quad 0 \leqslant t < t+h \leqslant t_\star, \qquad \text{(B.2)}$$

where ξ is a random vector with moments of a sufficiently high order and A is a d-dimensional vector function. We introduce (for simplicity) the equidistant partition of the time interval $[0, t_\star]$ into N parts with the step $h = t_\star/N$: $0 = t_0 < t_1 < \cdots < t_N = t_\star$, $t_{k+1} - t_k = h$. According to (B.2), we construct the sequence

$$X_0 = x, \qquad X_{k+1} = X_k + A(t_k, X_k, h; \xi_{k+1}), \quad k = 0, \ldots, N-1, \qquad \text{(B.3)}$$

where ξ_1 is independent of X_0 and ξ_{k+1} for $k > 0$ is independent of $X_0, \ldots, X_k, \xi_1, \ldots, \xi_k$.

We note that (B.3) contains both explicit and implicit one-step schemes. In explicit integration schemes the approximate solution at the next time step, X_{k+1}, can be computed explicitly from the previous time step value X_k. For implicit methods, $A(t, x, h; \xi)$ is a solution of an implicit relation with respect to x, i.e. implicit schemes in general require additional work.

We usually distinguish two types of convergence of numerical methods for SDEs: mean-square (also called strong) and weak [24]. Mean-square methods are used for direct simulation of SDE trajectories which, for example, can give information on the general behavior of a stochastic model. Weak methods are sufficient for evaluation of mean values and are simpler than mean-square ones. We say that the method (B.3) is weakly convergent with order $p > 0$ if

$$|\langle \varphi(X_N) \rangle - \langle \varphi(X(t_\star)) \rangle| \leqslant Ch^p \qquad \text{(B.4)}$$

for functions φ which, together with their derivatives of a sufficiently high order, have growth at infinity no faster than polynomial. If a method converges with an order p in the

mean-square sense, it also converges in the weak sense with order equal to or larger than p. The opposite is not true. Since weak methods suffice for computing averages, they are appropriate for the purposes of this paper.

To evaluate the expectation $\langle\varphi(X_N)\rangle$ on a computer, one can apply the Monte Carlo technique:

$$u \equiv \langle\varphi(X(t_\star))\rangle \simeq \bar{u} \equiv \langle\varphi(X_N)\rangle \simeq \hat{u} \equiv \frac{1}{M}\sum_{m=1}^{M}\varphi(X_N^{(m)}), \tag{B.5}$$

where $X_N^{(m)}$, $m = 1, \ldots, M$, are independent realizations of the random variable X_N. In (B.5) the first approximate equality involves the numerical integration error (cf (B.4)) and the error in the second approximate equality (the statistical error) comes from the Monte Carlo technique.

The error of the Monte Carlo method in (B.5) is evaluated by

$$\bar{\Delta} = c\frac{[\mathrm{Var}\{\varphi(\mathrm{X_N})\}]^{1/2}}{M^{1/2}},$$

where, for example, the values $c = 1, 2, 3$ correspond to the fiducial probabilities 0.68, 0.95, 0.997, respectively, with the practical implication that

$$\bar{u} \in \left(\hat{u} - \frac{c}{\sqrt{M}}\sqrt{\hat{v}}, \hat{u} + \frac{c}{\sqrt{M}}\sqrt{\hat{v}}\right), \qquad \hat{v} \equiv \frac{1}{M}\sum_{m=1}^{M}[\varphi({}_mX_N)]^2 - \hat{u}^2, \tag{B.6}$$

with probability 0.68 for $c = 1$, 0.95 for $c = 2$, and 0.997 for $c = 3$.

Now we assume that the solution of (B.1) is ergodic. In computing ergodic limits an additional error arises. We note that ergodic limits can be computed using ensemble averaging or time averaging. In the former case it follows from a relation of the form (A.1) for the solution $X(t)$ of (B.1) that for any $\varepsilon > 0$ there exists $t_a > 0$ such that for all $t_\star \geqslant t_a$

$$|\langle\varphi(X_x(t_\star))\rangle - \varphi^{\mathrm{erg}}| \leqslant \varepsilon. \tag{B.7}$$

Then we can use the following estimator for the ergodic limit φ^{erg}:

$$\varphi^{\mathrm{erg}} \approx \langle\varphi(X_x(t_\star))\rangle \approx \langle\varphi(X_N)\rangle \approx \hat{\varphi}^{\mathrm{erg}} \equiv \frac{1}{M}\sum_{m=1}^{M}\varphi(X_N^{(m)}), \tag{B.8}$$

where the first approximate equality corresponds to the time cut-off while the second one relates to the numerical integration error, and the third to the statistical error as before. In this ensemble averaging approach each of the errors is controlled by its own parameter (see [40]).

The time averaging approach to computing ergodic limits is based on a relation of the form (A.2). By approximating a single trajectory, one gets for a sufficiently large $\tilde{t}_\star$

$$\varphi^{\mathrm{erg}} \sim \frac{1}{\tilde{t}_\star}\int_0^{\tilde{t}_\star}\varphi(X_x(s))\,\mathrm{d}s \sim \check{\varphi}^{\mathrm{erg}} \equiv \frac{1}{L}\sum_{k=1}^{L}\varphi(X_k), \tag{B.9}$$

where $Lh = \tilde{t}_\star$. Let us emphasize that $\tilde{t}_\star$ in (B.9) is much larger than $t_\star$ in (B.8) because $\tilde{t}_\star$ should be such that it does not just ensure the distribution of $X(t)$ to be close to the invariant distribution (as is required from $t_\star$) but it should also guarantee smallness of the variance of $\check{\varphi}^{\mathrm{erg}}$ (see further details about computing ergodic limits in, for example, [40–42] and references therein).

References

[1] Landau L D and Lifshitz E M 1935 *Phys. Z. Sowjet.* **8** 153
[2] Akhiezer A I, Bar'yakhtar V G and Peletminskii S V 1968 *Spin Waves* (Amsterdam: North-Holland)
[3] Vonsovsky S V 1974 *Magnetism* (New York: Wiley)
[4] Aharoni A 2000 *Introduction to the Theory of Ferromagnetism* (Oxford: Oxford University Press)
[5] Žutić I, Fabian J and Das Sarma S 2004 *Rev. Mod. Phys.* **76** 323
[6] Gerrits Th, van den Berg H A M, Hohlfeld J, Bär L and Rasing Th 2002 *Nature* **418** 509
[7] Kimel A V, Kirilyuk A, Usachev P A, Pisarev R V, Balbashov A M and Rasing Th 2005 *Nature* **435** 655
[8] Koopmans B, Ruigrok J J M, Dalla Longa F and de Jonge W J M 2005 *Phys. Rev. Lett.* **95** 267207
[9] Melnikov A, Povolotskiy A and Bovensiepen U 2008 *Phys. Rev. Lett.* **100** 247401
[10] Novoselov K S, Geim A K, Dubonos S V, Hill E W and Grigorieva I V 2003 *Nature* **426** 812
[11] Dobrovitski V V, Katsnelson M I and Harmon B N 2003 *Phys. Rev. Lett.* **90** 067201
[12] Antropov V P, Katsnelson M I, van Schilfgaarde M and Harmon B N 1995 *Phys. Rev. Lett.* **75** 729
[13] Antropov V P, Katsnelson M I, Harmon B N, van Schilfgaarde M and Kuznecov D 1996 *Phys. Rev.* B **54** 1019
[14] Skubic B, Hellsvik J, Nordström L and Eriksson O 2008 *J. Phys.: Condens. Matter* **20** 315203
[15] Hellsvik J, Skubic B, Nordström L, Sanyal B, Eriksson O, Nordblad P and Svedlindh P 2008 *Phys. Rev.* B **78** 144419
[16] Skubic B, Peil O E, Hellsvik J, Nordblad P, Nordström L and Eriksson O 2009 *Phys. Rev.* B **79** 024411
[17] Nowak U 2001 *Annual Reviews of Computational Physics IX* ed D Stauffer (Singapore: World Scientific) p 105
[18] Kazantseva N, Nowak U, Chantrell R W, Hohlfeld J and Rebei A 2008 *Europhys. Lett.* **81** 27004
[19] d'Aquino M, Serpico C, Coppola G, Mayergoyz I D and Bertotti G 2006 *J. Appl. Phys.* **99** 08B905
[20] Hairer E, Lubich C and Wanner G 2002 *Geometric Numerical Integration: Structure Preserving Algorithms for Ordinary Differential Equations* (Berlin: Springer)
[21] Frank J, Huang W and Leimkuhler B 1997 *J. Comput. Phys.* **133** 160
[22] Arponen T and Leimkuhler B 2004 *BIT Numer. Math.* **44** 403
[23] Milstein G N, Repin Yu M and Tretyakov M V 2002 *SIAM J. Numer. Anal.* **40** 1583
[24] Milstein G N and Tretyakov M V 2004 *Stochastic Numerics for Mathematical Physics* (Berlin: Springer)
[25] Davidchack R L, Handel R and Tretyakov M V 2009 *J. Chem. Phys.* **130** 234101
[26] Krech M, Bunker A and Landau D P 1998 *Comput. Phys. Commun.* **111** 1
[27] Steinigeweg R and Schmidt H J 2006 *Comput. Phys. Commun.* **174** 853
[28] Banas L 2005 *Lecture Notes in Computer Science: Numerical Analysis and its Applications* ed Z Li *et al* (Berlin: Springer) p 158

[29] Kubo R and Hashitsume N 1970 *Prog. Theor. Phys. Suppl.* **46** 210
[30] Brown W F 1963 *Phys. Rev.* **130** 1677
[31] Gardiner C W 2004 *Handbook of Stochastic Methods* (Berlin: Springer)
[32] Stratonovich R L 1968 *Conditional Markov Processes and their Application to the Theory of Optimal Control* (Amsterdam: Elsevier)
[33] Hasminskii R Z 1980 *Stochastic Stability of Differential Equations* (Groningen: Sijthoff & Noordhoff)
[34] Milstein G N and Tretyakov M V 1994 *J. Stat. Phys.* **77** 691
[35] Milstein G N and Tretyakov M V 1997 *SIAM J. Numer. Anal.* **34** 2142
[36] Shubin S and Zolotukhin M 1936 *Zh. Eksp. Teor. Fiz.* **6** 105
[37] Fisher M E 1964 *Am. J. Phys.* **32** 343
[38] Soize C 1994 *The Fokker–Planck Equation for Stochastic Dynamical Systems and its Explicit Steady State Solutions* (Singapore: World Scientific)
[39] Garcıa Palacios J L and Lazaro F J 1998 *Phys. Rev.* B **58** 14937
[40] Milstein G N and Tretyakov M V 2007 *Physica* D **229** 81
[41] Mattingly J C, Stuart A M and Tretyakov M V 2010 Convergence of numerical time-averaging and stationary measures via Poisson equations *SIAM J. Numer. Anal.* at press (arXiv:0908.4450v2)
[42] Talay D 1990 *Stoch. Stoch. Rep.* **29** 13